Preprints of the 21st IFAC World Congress (Virtual)
Berlin, Germany, July 12-17, 2020

# Event-triggered control co-design for rational systems ⋆

**L. G. Moreira** * **J. M. Gomes da Silva Jr.** ** **D. Coutinho** ***
**S. Tarbouriech** ****

* *Inst. Fed. de Educ., Ciência e Tecnol. Sul-rio-grandense, Brazil. (e-mail: lucianomoreira@charqueadas.ifsul.edu.br).*
** *Universidade Federal do Rio Grande do Sul, Brazil. (e-mail: jmgomes@ufrgs.br)*
*** *Universidade Federal de Santa Catarina, Brazil. (e-mail: daniel.coutinho@ufsc.br)*
**** *LAAS-CNRS, Université de Toulouse, France. (e-mail: sophie.tarbouriech@laas.fr)*

**Abstract:** This work deals with the problem of designing stabilizing event-triggered state-feedback controllers for rational systems. Using differential algebraic representations and Lyapunov theory techniques, LMI-based conditions are derived to ensure regional asymptotic stability of the origin. These conditions are then cast into a convex optimization problem to the co-design of the event generator parameters and the state-feedback gain in order to reduce the controller updates while ensuring the asymptotic stability of the origin with respect to a given set of admissible initial conditions. The proposed methodology is illustrated by means of a numerical example.

*Keywords:* Event-triggered control; Nonlinear Systems; Control system synthesis; Co-design; Networked Control Systems.

## 1. INTRODUCTION

Event-triggered control (ETC) is a control paradigm for which the feedback data is sampled and/or the control is updated only when a certain criterion (based on the system behavior) is verified. As a result, a smaller number of control updates is typically needed when compared to the periodic sampling/control updating paradigm (Abdelrahim et al., 2015) which in a networked control setup represents less transmissions across the network, reducing bandwidth and energy consumption (see, e.g., Heemels et al. (2012), Abdelrahim et al. (2015) and the references cited therein).

Basically, two design approaches for event-triggered control are available in the literature, namely, emulation design and co-design. The emulation design approach assumes that a stabilizing controller has been designed not taking into account the event-triggering strategy and then the event generator is designed in order to guarantee the closed-loop stability. In contrast, the controller and event generator are simultaneously designed in the co-design approach.

The emulation approach for linear systems is addressed in various works. For instance, Heemels et al. (2012) presents the ETC paradigm and also addresses self-triggered control. In Donkers and Heemels (2012), decentralized triggering mechanisms are considered. Output-feedback and time-delay techniques are considered in Selivanov and Fridman (2016). More recently, Cuenca et al. (2019) proposed emulation designed ETC to control unmanned autonomous vehicles modeled as linear systems and Abdelrahim et al. (2019) addressed output-based ETC considering distributed sensors and asynchronous transmission of their data.

In the context of nonlinear systems, Abdelrahim et al. (2016) proposes an emulation approach based on a hybrid system framework assuming that a global stabilizing output feedback control law is given *a priori*. In this case, a timer is considered to guarantee a minimum inter-event time and avoid Zeno behavior. PI controllers for linear plants subject to saturation of the control input are considered in Moreira et al. (2019a), which also addresses the co-design case. Emulation approach considering Lure type systems with sector-bounded nonlinearities in the inputs are considered in Tarbouriech et al. (2017). Wang et al. (2018) study the stabilization of perturbed nonlinear systems using output-based periodic event-triggered controllers (PETC) and a hybrid systems framework in an emulation-based setting. Particular classes of nonlinear systems are addressed in an emulation context in Peralez et al. (2018), which uses high-gain techniques to achieve output-feedback stabilization, and in Xing et al. (2019),

⋆ This study was financed in part by the Coordenação de Aperfeiçoamento de Pessoal de Nível Superior - Brazil (CAPES) - Finance Code 001 (PROEX, SticAmSud 88881.143275/2017-01); CNPq, Brazil (grants PQ 307449/2019-0, Univ-422992/2016-0 and PQ-302690/2018-2); IFSUL, Brazil (Project PD00190519/011); STIC AMSuD 18-STIC-01, CoDysco2 - France; ANR project HANDY 18-CE40-0010.

which proposes a 1-bit encoding-decoding procedure to further reduce the bandwidth consumption, but allowing to achieve only practical stability.

Regarding the co-design for linear systems, we can cite Heemels et al. (2013), which addresses PETC and Abdelrahim et al. (2018), which considers sensor and actuator transmissions at different times and handles external disturbances. The co-design for nonlinear systems is addressed, for instance, in Groff et al. (2016); Moreira et al. (2019a); Seuret et al. (2016), which consider linear systems with saturation of control inputs, Li and Huang (2017); Jia et al. (2014) considering Takagi-Sugeno (T-S) models for the nonlinearities and Moreira et al. (2019b) which considers cone-bounded nonlinearities and a nonlinear state observer to estimate non-measurable state variables.

It should be highlighted that many nonlinear plants of interest admit rational models, as, for instance, mobile robots modeled via quartenions (Tayebi and McGilvray, 2006), generic biological systems (Wu and Mu, 2009) and bio-reactors (Campestrini et al., 2014). Besides that, the class of rational systems encompasses the polynomial systems and high-order Taylor series approximations of other classes of nonlinear systems. Motivated by that, in our previous work (Moreira et al., 2017), we addressed the emulation design of event-triggered controllers for rational nonlinear systems. The current paper can be viewed as a complementary version of Moreira et al. (2017), in the sense it tackles the co-design case.

The main challenge in the co-design case is to obtain tractable stability conditions. As in Moreira et al. (2017), differential algebraic representations (DARs) (Trofino, 2000; Coutinho et al., 2004) allow us to model the nonlinearities in a convenient way. However, differently from the emulation case, here it is not possible to use the Finsler Lemma to obtain stability conditions in LMI form. Hence, alternative techniques are employed to achieve that goal. The conditions are then cast into a convex optimization problem proposed as means of synthesizing the event-triggered controller aiming at a small number of events while keeping the closed-loop system asymptotically stable for all initial conditions in a given admissible set.

**Notation**. $\mathbb{R}$, $\mathbb{R}^n$ and $\mathbb{R}^{n\times m}$ represent respectively the set of real numbers, $n$-dimensional real vectors and $n\times m$ real matrices. For a real matrix $A$, $A'$ denotes its transpose, $\mathrm{He}\{A\} = A + A'$, $\mathrm{tr}(A)$ is the trace of $A$ and $A > 0$ states that $A$ is symmetric and positive definite. For $B \in \mathbb{R}^{n\times n}$, $\lambda_{min}(B)$ and $\lambda_{max}(B)$ denote respectively the smallest and largest eigenvalues of $B$. The symbol $*$ stands for symmetric blocks within a matrix. $\mathrm{diag}(X, Y)$ denotes the block-diagonal matrix composed by the blocks $X$ and $Y$. 0 is used to represent matrices of null entries of appropriate dimensions. $\|\cdot\|$ denotes the Euclidean norm and $|\cdot|$ denotes the absolute value. $\mathcal{E}(P) = \{\xi \in \mathbb{R}^n : \xi' P \xi \leq 1\}$ denotes an ellipsoid whose shape and size are defined by the matrix $P = P' > 0 \in \mathbb{R}^{n\times n}$. For a polytope $\mathcal{B}$, $\mathcal{V}(\mathcal{B})$ denotes the set of all vertices of $\mathcal{B}$.

## 2. PROBLEM STATEMENT

Consider the following continuous-time plant:

$$\dot{x}(t) = f(x(t)) + g(x(t))u(t) \tag{1}$$

where $x(t) \in \mathcal{B}_x \subset \mathbb{R}^n$ is the state vector; $u(t) \in \mathbb{R}^m$ is the input; $f(x)$ and $g(x)$ are regular rational functions for all $x \in \mathcal{B}_x$ with $f(0) = 0$; and $\mathcal{B}_x$ is a compact set containing the state space origin to be defined later in this paper. We assume, without loss of generality, that $x = 0$ is the equilibrium point of interest.

Considering an event-triggered control strategy, we suppose that at instants $t = t_k,\ k = 0, 1, 2, \ldots$, determined by an event generator, a sample of the plant state is considered to update the control signal $u(t)$. Between two event instants, the controller input is held constant by means of a zero-order holder. We assume $t_0 = 0$. Therefore, the closed-loop system considering a static state-feedback controller can be represented by the equation:

$$\begin{cases} \dot{x}(t) = f(x(t)) + g(x(t))u(t) \\ u(t) = Kx(t_k) \qquad\qquad \forall t \in [t_k, t_{k+1}) \end{cases} \tag{2}$$

Defining, as proposed in Tabuada (2007), the error signal $\delta(t) = x(t_k) - x(t)$, we can rewrite (2) as:

$$\begin{aligned} \dot{x}(t) &= f(x(t)) + g(x(t))K(x(t) + \delta(t)) \\ &= f(x(t)) + g(x(t))Kx(t) + g(x(t))K\delta(t) \\ &\qquad\qquad \forall t \in [t_k, t_{k+1}) \end{aligned} \tag{3}$$

Note that at the instants $t = t_k$, $\forall k \in \mathbb{N}$, the value of $\delta(t)$ is reset to zero.

In this work, we aim at simultaneously designing the controller gain matrix $K$ and an event-triggering strategy leading to a small number of control updates. To this end, we consider the triggering strategy of Moreira et al. (2017), that can expressed by the following rule to determine the event instants:

$$t_{k+1} = \min\{t > t_k \mid \delta'(t)Q_\delta\delta(t) - x'(t)Q_x x(t) > 0\} \tag{4}$$

$Q_\delta$ and $Q_x$ are symmetric positive definite matrices of appropriate dimensions that act as weights. The "larger" $Q_x$ and the "smaller" $Q_\delta$ are, the more we let the current state deviate from the last sampled one before a new event is generated and thus less control updates are expected. This rule is an extension of the event-triggering criterion originally introduced in Tabuada (2007), in the sense that it can be recovered by taking $Q_\delta = I$ and $Q_x = \sigma I$.

Then, the problem to be addressed in this paper can be stated as follows:

*Problem 1.* Co-design the gain $K$ and the triggering function parameters $Q_x$ and $Q_\delta$ such that the local asymptotic stability of the origin of the closed-loop system (2) with the control update instants given by the rule (4) is ensured for a given set $\mathcal{X}_0$ of admissible initial conditions while aiming at a small number of events.

## 3. MAIN RESULTS

In this section we formulate stability conditions to address Problem 1. Let us start by considering that our region of interest is defined by the following symmetric polytope of $2n_f$ faces:

$$\mathcal{B}_x = \{x \in \mathbb{R}^n : |h_i' x| \leq 1,\ h_i \in \mathbb{R}^n,\ i = 1, \ldots, n_f\} \tag{5}$$

which can be alternatively defined in terms of the convex hull of $n_v$ vertices, i.e., $\mathcal{B}_x = \mathrm{Co}\{v_1, \ldots, v_{n_v}\}$ with $v_i \in \mathbb{R}^n$, $i = 1, \ldots, n_v$.

To obtain tractable conditions, we use the concept of differential algebraic representations (DARs), as proposed in Trofino (2000). A DAR for system (3) is given as follows:

$$\begin{cases} \dot{x} = (A_1(x) + A_3(x)K)\,x + A_2(x)\xi(x,\delta) + A_3(x)K\delta \\ 0 = (\Omega_1(x) + \Omega_3(x)K)\,x + \Omega_2(x)\xi(x,\delta) + \Omega_3(x)K\delta \end{cases} \tag{6}$$

with $\xi(x,\delta) \in \mathbb{R}^q$ being an auxiliary variable containing nonlinear terms of both $f(x)$ and $g(x)K(x+\delta)$. Furthermore, $A_1(x) \in \mathbb{R}^{n\times n}$, $A_2(x) \in \mathbb{R}^{n\times q}$, $A_3(x) \in \mathbb{R}^{n\times m}$, $\Omega_1(x) \in \mathbb{R}^{q\times n}$, $\Omega_2(x) \in \mathbb{R}^{q\times q}$ and $\Omega_3(x) \in \mathbb{R}^{q\times m}$ are affine matrix functions of $x$. We have omitted the time dependency here to simplify notation. It is assumed that (3) can be recovered from (6) by eliminating $\xi(x,\delta)$, which implies that $\Omega_2(x)$ needs to be full column rank $\forall x \in \mathcal{B}_x$. Notice that, since $f(x)$ and $g(x)$ are rational functions of the state, $f(x) + g(x)K(x+\delta)$ is rational on $x$ and linear on $\delta$, and the decomposition of (3) in the form (6) is always possible. It should be pointed out, however, that the decomposition is in general not unique (Coutinho et al., 2004; Trofino, 2000).

Based on the DAR (6), the next theorem provides conditions to compute the gain matrix $K$ and the matrices $Q_x$ and $Q_\delta$ such that the origin of the closed-loop system (2) under the event-triggering strategy given by (4) is regionally asymptotically stable.

*Theorem 1.* Consider the nonlinear system in (1), its DAR in (6) and the event generator as in (4). Let $\mathcal{B}_x$ be a given polytope as in (5). If there exist constant symmetric positive definite matrices $\bar{Q}_x \in \mathbb{R}^{n\times n}$, $\bar{Q}_\delta \in \mathbb{R}^{n\times n}$, $N_2 \in \mathbb{R}^{n\times n}$ and generic constant matrices $Y \in \mathbb{R}^{n\times m}$, $N_1 \in \mathbb{R}^{n\times n}$, $N_3 \in \mathbb{R}^{q\times q}$, such that the following LMIs are satisfied $\forall v \in \mathcal{V}(\mathcal{B}_x)$:

$$\begin{bmatrix} \psi_a & \psi_b & \psi_c & \psi_d & N_2 \\ * & \psi_e & \psi_f & \psi_d & 0 \\ * & * & \psi_g & \psi_h & 0 \\ * & * & * & -\bar{Q}_\delta & 0 \\ * & * & * & * & -\bar{Q}_x \end{bmatrix} < 0 \tag{7}$$

$$\begin{bmatrix} N_2 & N_2 h_i \\ * & 1 \end{bmatrix} > 0, \quad i = 1,\dots,n_f \tag{8}$$

where

$\psi_a = \mathrm{He}\{A_1(v)N_2 + A_3(v)Y'\}$, $\psi_b = N_2A_1'(v) + YA_3'(v)$,
$\psi_c = A_2(v)N_3' + N_2\Omega_1'(v) + Y\Omega_3'(v)$, $\psi_d = A_3(v)Y'$,
$\psi_e = -\mathrm{He}\{N_1\}$, $\psi_f = A_2(v)N_3'$, $\psi_g = \mathrm{He}\{\Omega_2(v)N_3'\}$,
$\psi_h = \Omega_3(v)Y'$

then, the sampling strategy given by (4) with $Q_x = \bar{Q}_x^{-1}$, $Q_\delta = N_2^{-1}\bar{Q}_\delta N_2^{-1}$ and $K = YN_2^{-1}$ renders the origin of the closed-loop system (2) asymptotically stable and $\mathcal{E}(N_2^{-1}) = \{x \in \mathbb{R}^n : x'N_2^{-1}x \le 1\}$ is included in its region of attraction, i.e. $\forall x(0) \in \mathcal{E}(N_2^{-1})$, $x(t) \to 0$ when $t \to \infty$.

**Proof.**

We can rearrange the terms of the representation (6) as:

$$\begin{cases} -\dot{x} + (A_1 + A_3K)x + A_2\xi + A_3K\delta = 0 \\ (\Omega_1 + \Omega_3K)x + \Omega_2\xi + \Omega_3K\delta = 0 \end{cases} \tag{9}$$

where we omitted the dependencies of the matrices on $x$ and $\delta$ for notation simplicity. From this, the following relations are verified along system (2) trajectories, for any matrices $M_1$, $M_2$ and $M_3$ of appropriate dimensions:

$$\begin{aligned} \beta_1 &= \dot{x}'M_1\big(-\dot{x} + (A_1 + A_3K)x + A_2\xi + A_3K\delta\big) = 0 \\ \beta_2 &= x'M_2\big(-\dot{x} + (A_1 + A_3K)x + A_2\xi + A_3K\delta\big) = 0 \\ \beta_3 &= \xi'M_3\big((\Omega_1 + \Omega_3K)x + \Omega_2\xi + \Omega_3K\delta\big) = 0 \end{aligned} \tag{10}$$

Considering a quadratic Lyapunov function $V(x) = x'Px$, with $P$ symmetric positive definite, defining the vector $\zeta = [x'\ \dot{x}'\ \xi'\ \delta']'$, taking into account the relations in (10), the time-derivative $\dot{V}(x)$ can be written as:

$$\begin{aligned} \dot{V}(x) &= \dot{V}(x) + 2\beta_1 + 2\beta_2 + 2\beta_3 = \\ &= \zeta' \begin{bmatrix} \psi_1 & \psi_2 & \psi_3 & M_2A_3K \\ * & -\mathrm{He}\{M_1\} & M_1A_2 & M_1A_3K \\ * & * & \mathrm{He}\{M_3\Omega_2\} & M_3\Omega_3K \\ * & * & * & 0 \end{bmatrix} \zeta \end{aligned} \tag{11}$$

with

$$\begin{aligned} \psi_1 &= \mathrm{He}\{M_2(A_1 + A_3K)\} \\ \psi_2 &= P + (A_1 + A_3K)'M_1' - M_2 \\ \psi_3 &= M_2A_2 + (\Omega_1 + \Omega_3K)'M_3' \end{aligned}$$

Hence, from (11), if the following relation is satisfied:

$$\begin{bmatrix} \psi_1 + Q_x & \psi_2 & \psi_3 & M_2A_3K \\ * & -\mathrm{He}\{M_1\} & M_1A_2 & M_1A_3K \\ * & * & \mathrm{He}\{M_3\Omega_2\} & M_3\Omega_3K \\ * & * & * & -Q_\delta \end{bmatrix} < 0 \tag{12}$$

we have $\dot{V}(x) < \delta'Q_\delta\delta - x'Q_xx$ along the trajectories of the system. Since from (4) it follows that $\delta'Q_\delta\delta - x'Q_xx < 0$ for $t \in (t_k, t_{k+1})$, we conclude that $\dot{V}(x) < 0$ in this time interval. Moreover, for $t = t_k$, we have $\delta = 0$ and thus it also follows that $\dot{V}(x(t_k)) < -x'(t_k)Q_xx(t_k) < 0$.

Suppose now that $M_1, M_2, M_3$ are non-singular matrices, and define $N_1 = M_1^{-1}, N_2 = M_2^{-1}, N_3 = M_3^{-1}$. Pre- and post-multiplying (12) by $\mathrm{diag}(N_2, N_1, N_3, N_2)$ and $\mathrm{diag}(N_2', N_1', N_3', N_2')$ respectively, we obtain:

$$\begin{bmatrix} \psi_4 & \psi_5 & \psi_6 & A_3KN_2' \\ * & -\mathrm{He}\{N_1\} & A_2N_3' & A_3KN_2' \\ * & * & \mathrm{He}\{\Omega_2N_3'\} & \Omega_3KN_2' \\ * & * & * & -N_2Q_\delta N_2' \end{bmatrix} < 0 \tag{13}$$

with

$$\begin{aligned} \psi_4 &= \mathrm{He}\{(A_1 + A_3K)N_2'\} + N_2Q_xN_2' \\ \psi_5 &= N_2PN_1' + N_2(A_1 + A_3K)' - N_1' \\ \psi_6 &= A_2N_3' + N_2(\Omega_1 + \Omega_3K)' \end{aligned}$$

Applying the Schur's complement to $\psi_4$, making the additional restriction $P = M_2$ (which implies $N_2PN_1' = N_1'$ and $N_2 = N_2' > 0$) and applying the changes of variables $Y = N_2K'$, $\bar{Q}_\delta = N_2Q_\delta N_2$ we obtain the relation (7) with $v = x$. Since the left-hand side matrix in (7) is affine on $v$, by convexity arguments, if relation (7) is verified at the vertices of $\mathcal{B}_x$, we can conclude that $\dot{V}(x) < 0$, $\forall x \in \mathcal{B}_x$.

In this case, any level set of the Lyapunov function $V(x) = x'Px = x'N_2^{-1}x$ included in $\mathcal{B}_x$ is a contractive and invariant set for the trajectories of the closed-loop system. Note now that (8) ensures that the level set $\mathcal{E}(N_2^{-1}) \subset \mathcal{B}_x$, i.e. $\forall x \in \mathcal{E}(N_2^{-1})$, it follows that $\lim_{t\to\infty} x(t) = 0$, which concludes the proof. □

*Remark 1.* Theorem 1 also guarantees that the control gain $K$ asymptotically stabilizes the closed-loop system origin under a continuous-time control law $u(t) = Kx(t)$.

Furthermore, $\mathcal{E}(N_2^{-1})$ is included in the region of attraction of the origin. This follows from the fact that the continuous-time system corresponds to (6) with $\delta = 0$, and in this case, conditions (7) and (8) guarantee that $\dot{V}(x) < -x'Q_x x < 0$, $\forall t \geq 0$, $\forall x(0) \in \mathcal{E}(N_2^{-1})$.

*Remark 2.* The LMIs (7)-(8) need to be verified only at the vertices of the region $\mathcal{B}_x$ to ensure that the Lyapunov function is strictly decreasing for all $x \in \mathcal{B}_x$ and thus ensure the asymptotic stability of the origin. Note that if the origin is stabilizable by a linear state feedback, then for a sufficient small $\mathcal{B}_x$ the LMIs will in general be feasible. On the other hand, as we increase $\mathcal{B}_x$ we can ensure the stability for larger sets of admissible states. The appropriate choice and parameterization of $\mathcal{B}_x$ are discussed in section 4.

To be of practical use, the triggering strategy cannot lead to Zeno solutions (Tabuada, 2007; Heemels et al., 2012). Since the strategy considered here is the same as in Moreira et al. (2017), we can leverage Theorem 2 presented in that paper to ensure a minimum time between events, which guarantees that Zeno behavior never occurs with the proposed approach.

*Theorem 2.* (Moreira et al. 2017). The inter-sampling times implicitly defined by the triggering rule (4) are lower-bounded.

**Proof.** The proof is identical to the one presented in (Moreira et al., 2017, Theorem 2) and is omitted here due to space limitations. It can be obtained from the authors. □

## 4. CONTROLLER TUNNING

In this section we propose an optimization problem as means to simultaneously compute the parameters $K$, $Q_x$ and $Q_\delta$ aiming at a small number of events when the event-triggering strategy given by (4) is considered.

Suppose that the region of initial states $\mathcal{X}_0$ where we want to guarantee the convergence to the origin is defined by $\mathcal{X}_0 = \{x \in \mathbb{R}^n : x'P_0x \leq 1\} \subset \mathcal{B}_x$, with $P_0 \in \mathbb{R}^{n\times n}$ a given symmetric positive definite matrix. The stability problem can then be translated into ensuring that $\mathcal{X}_0 \subset \mathcal{E}(N_2^{-1})$ and that the stability conditions of Theorem 1 are fulfilled. To ensure $\mathcal{X}_0 \subset \mathcal{E}(N_2^{-1})$, we can use the constraint $N_2^{-1} < P_0$, or, more appropriately, $N_2 > P_0^{-1}$.

To reduce the control updates, we aim at finding $Q_x$ as "large" as possible and $Q_\delta$ as "small" as possible, while still satisfying the stability conditions. From Theorem 2, in fact we aim at minimizing the ratio $\frac{\lambda_{\max}(Q_\delta)}{\lambda_{\min}(Q_x)}$. However, this represents a nonlinear objective function. Moreover, the triggering function parameters $Q_x$ and $Q_\delta$ do not appear explicitly in the stability conditions. Therefore, approximations need to be considered to define a suitable optimization problem. Since $\bar{Q}_x = Q_x^{-1}$ and $\bar{Q}_\delta = N_2 Q_\delta N_2$ appear in the conditions, we propose to minimize $\mathrm{tr}(\bar{Q}_\delta + \bar{Q}_x)$ as an approximation, leading to the following optimization problem:

$$\begin{aligned} &\min(\mathrm{tr}(\bar{Q}_\delta + \bar{Q}_x)) \\ &\quad \text{subject to: (7), (8), } N_2 > P_0^{-1} \end{aligned} \tag{14}$$

Table 1. Linear search on $\mathcal{B}_x$ size – small $\mathcal{X}_0$

| | $\rho$ | $\mathrm{tr}(\bar{Q}_\delta + \bar{Q}_x)$ |
|---|---|---|
| | 0.15 | 1.0329 |
| | 0.30 | 0.21823 |
| * | 0.31 | 0.21822 |
| | 0.32 | 0.21891 |
| | 0.35 | 0.2246 |
| | 0.60 | 0.37405 |

Notice that the choice of $\mathcal{B}_x$ impacts the results obtained with this optimization problem. For this reason, one should parameterize $\mathcal{B}_x$ (e.g. as a symmetric polytope around the origin) and execute a search on the parameter(s), i.e. solve optimization problem (14) for each value of the parameter(s), looking for the minimum value of the objective function among them and taking the values of $Q_\delta$ and $Q_x$ obtained for this minimum value. It should be highlighted that (14) is a convex optimization problem, since (7) and (8) are LMIs. Therefore, there exist efficient methods to solve it.

## 5. NUMERICAL EXAMPLE

In this example, we consider the following rational plant:

$$\begin{cases} \dot{x}_a(t) = \dfrac{1 + x_a^2(t)}{2} x_b(t) \\ \dot{x}_b(t) = \dfrac{2}{1 + x_a^2(t)} x_a(t) - x_b(t) - \dfrac{1 - x_a^2(t)}{1 + x_a^2(t)} u(t) \end{cases} \tag{15}$$

where $x = [x_a \ x_b]' \in \mathbb{R}^2$ is the state of the plant. This system models the rotational motion of a cart with an inverted pendulum after applying some variable changes to convert the system from transcendental into rational (see Coutinho and Gomes da Silva Jr. (2010) for the details).

We consider a DAR (6), with

$$\xi(x, \delta) = \left[ x_a x_b \ \ \tfrac{x_a}{1+x_a^2} \ \ \tfrac{x_a^2}{1+x_a^2} \ \ \tfrac{K(x+\delta)}{1+x_a^2} \ \ \tfrac{x_a K(x+\delta)}{1+x_a^2} \right]'$$

and the following matrices:

$$A_1 = \begin{bmatrix} 0 & 0.5 \\ 0 & -1 \end{bmatrix}, \ A_2 = \begin{bmatrix} 0.5x_a & 0 & 0 & 0 & 0 \\ 0 & 2 & 0 & 0 & 2x_a \end{bmatrix}, \ A_3 = [0 \ -1]'$$

$$\Omega_1 = \begin{bmatrix} -x_b & 0 \\ -1 & 0 \\ 0 & 0 \\ 0 & 0 \\ 0 & 0 \end{bmatrix}, \ \Omega_2 = \begin{bmatrix} 1 & 0 & 0 & 0 & 0 \\ 0 & 1 & x_a & 0 & 0 \\ 0 & -x_a & 1 & 0 & 0 \\ 0 & 0 & 0 & 1 & x_a \\ 0 & 0 & 0 & -x_a & 1 \end{bmatrix}, \ \Omega_3 = \begin{bmatrix} 0 \\ 0 \\ 0 \\ -1 \\ 0 \end{bmatrix}.$$

Choosing $\mathcal{X}_0 = \{x \in \mathbb{R}^2 : x'P_0x \leq 1\}$, with $P_0 = 50I$, considering a symmetric polytope $\mathcal{B}_x$ with sides of length $\rho$ (that is, $\mathcal{B}_x$ defined as in (5) with $h_1 = \rho^{-1}[1 \ 0]$ and $h_2 = \rho^{-1}[0 \ 1]$) and solving the optimization problem (14) for various values of $\rho$ (i.e., various sizes of $\mathcal{B}_x$), we obtain the results shown in Table 1. The asterisk marks the line corresponding to the best value found for the objective function, corresponding to $\rho = 0.31$. With $\rho = 0.31$, the optimization problem yields:

$$Q_x = \begin{bmatrix} 18 & 7.63 \\ 7.63 & 16.3 \end{bmatrix} \qquad Q_\delta = \begin{bmatrix} 112 & 51.5 \\ 51.5 & 23.6 \end{bmatrix}$$

$$P = N_2^{-1} = \begin{bmatrix} 46.1 & 12 \\ 12 & 13.5 \end{bmatrix} \quad K = [4.17 \ 1.91]$$

Results of simulations considering the corresponding closed-loop system are depicted in figures 1 and 2. The

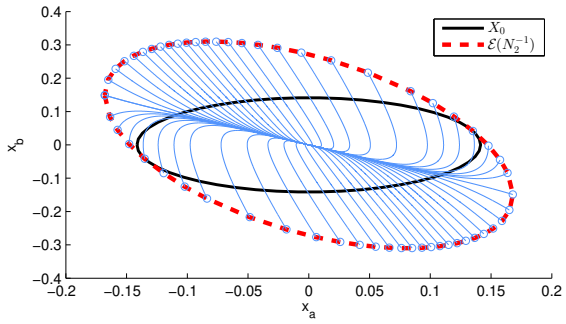


Fig. 1. $\mathcal{X}_0$, $\mathcal{E}(N_2^{-1})$ and some trajectories – $P_0 = 50I$.

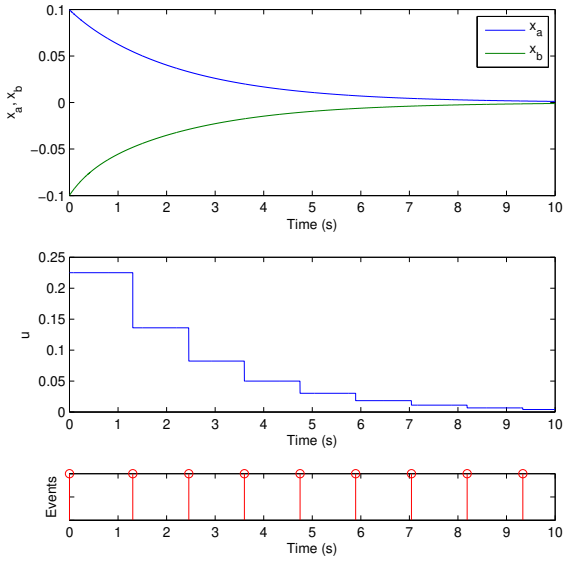


Fig. 2. Simulation – $P_0 = 50I$.

borders of the sets $\mathcal{X}_0$ and $\mathcal{E}(N_2^{-1})$ are shown in black solid line and in red dashed line, respectively, in Figure 1. It can be seen that $\mathcal{E}(N_2^{-1}) \supset \mathcal{X}_0$ as expected and the trajectories starting inside $\mathcal{E}(N_2^{-1})$ converge to the origin. Figure 2 depicts the time evolution of the state considering an initial condition $x(0) = [0.1 \ \ -0.1]'$, the control signal and the events activity in the plots at the top, middle and bottom, respectively. A total of 9 events were generated in the time interval $[0, 10]$. The minimum inter-event time observed in this simulation was 1.145 s.

Considering now a larger set $\mathcal{X}_0$, with $P_0 = 5I$ and solving optimization problem (14) for various values of $\rho$, we obtain the results shown in Table 2. As in the previous examples, an asterisk marks the line corresponding to the best objective function value found, in this case, for $\rho = 0.64$. With $\rho = 0.64$, the optimization problem yields:

$$Q_x = \begin{bmatrix} 0.755 & 1.34 \\ 1.34 & 2.81 \end{bmatrix} \qquad Q_\delta = \begin{bmatrix} 41.2 & 75.6 \\ 75.6 & 139 \end{bmatrix}$$

$$P = N_2^{-1} = \begin{bmatrix} 3.65 & 1.59 \\ 1.59 & 3.13 \end{bmatrix} \qquad K = [33.2 \ \ 61]$$

Figure 3 depicts, as in the previous case, the set $\mathcal{X}_0$ in black solid line, the set $\mathcal{E}(N_2^{-1})$ in red dashed line and some trajectories of the closed-loop system for initial conditions inside $\mathcal{E}(N_2^{-1})$. Just as in the previous case, $\mathcal{E}(N_2^{-1}) \supset \mathcal{X}_0$ and the trajectories converge to the origin as required. In Figure 4, the top plot shows the time evolution of a

Table 2. Linear search on $\mathcal{B}_x$ size – large $\mathcal{X}_0$

| | $\rho$ | $\mathrm{tr}(\bar{Q}_\delta + \bar{Q}_x)$ |
|---|---|---|
| | 0.53 | 209.09 |
| | 0.63 | 24.489 |
| * | 0.64 | 24.456 |
| | 0.65 | 24.575 |
| | 0.70 | 27.286 |
| | 0.90 | 176.08 |

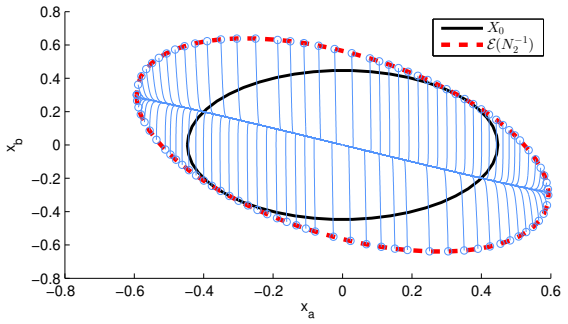


Fig. 3. $\mathcal{X}_0$, $\mathcal{E}(N_2^{-1})$ and some trajectories – $P_0 = 5I$.

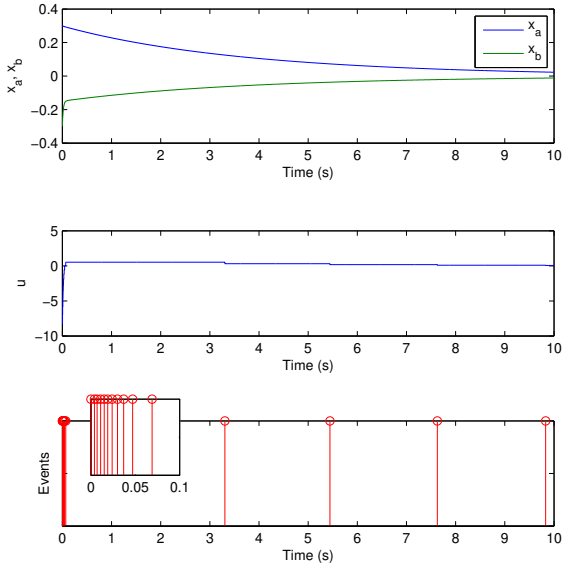


Fig. 4. Simulation – $P_0 = 5I$.

simulation with $x(0) = [0.3 \ \ -0.3]'$, the middle plot shows the control action and the bottom plot shows the events (with a zoom at the initial instants of time depicted in the small box). A total of 15 events were generated in the time interval $[0, 10]$ and the minimum inter-event time was 3 ms. We can see that when we strive for ensuring stability for a larger region of initial states, the event-triggering strategy becomes less effective and the number of events increases. This can be intuitively explained by the fact that starting farther away from the origin, a more effective control is needed, which implies the necessity of more control updates in the initial instants (i.e., when the state is still far from the origin).

## 6. CONCLUDING REMARKS

In this work we have proposed a method to design event-triggered control systems for continuous-time rational non-

linear plants. The method is based on the use of a class of differential algebraic representations and guarantees regional asymptotic stability of the origin for a given set of initial conditions. The derived stability conditions are cast in terms of a finite set of LMI constraints and a convex optimization problem is proposed to simultaneously compute the control law and the event-triggering function parameters aiming at a small number of control signal updates. Numerical experiments considering a rational system illustrated the effectiveness of the method and highlighted the relation between the expected number of samples and the size of the region of initial conditions where the asymptotic stability is to be ensured.

## REFERENCES

Abdelrahim, M., Postoyan, R., Daafouz, J., and Nešić, D. (2015). Input-to-state stabilization of nonlinear systems using event-triggered output feedback controllers. In *Proceedings of the European Control Conference*, 2180–2185. Linz.

Abdelrahim, M., Postoyan, R., Daafouz, J., Nešić, D., and Heemels, W.P.M.H. (2018). Co-design of output feedback laws and event-triggering conditions for the $\mathcal{L}_2$-stabilization of linear systems. *Automatica*, 87, 337 – 344.

Abdelrahim, M., Postoyan, R., Daafouz, J., and Nešić, D. (2016). Stabilization of nonlinear systems using event-triggered output feedback controllers. *IEEE Trans. Autom. Control*, 61(9), 2682–2687.

Abdelrahim, M., Sebastiaan Dolk, V., and Heemels, W. (2019). Event-triggered quantized control for input-to-state stabilization of linear systems with distributed output sensors. *IEEE Trans. Autom. Control*, 1–16.

Campestrini, L., Eckhard, D., Rui, R., and Bazanella, A.S. (2014). Identifiability analysis and prediction error identification of anaerobic batch bioreactors. *Journal of Control, Automation and Electrical Systems*, 25(4), 438–447.

Coutinho, D.F., Bazanella, A.S., Trofino, A., and Silva, A.S. (2004). Stability analysis and control of a class of differential-algebraic nonlinear systems. *Int. J. Robust Nonlinear Control*, 14(16), 1301–1326.

Coutinho, D.F. and Gomes da Silva Jr., J.M. (2010). Computing estimates of the region of attraction for rational control systems with saturating actuators. *IET Control Theory Applications*, 4(3), 315–325.

Cuenca, A., Antunes, D.J., Castillo, A., García, P., Khashooei, B.A., and Heemels, W.P.M.H. (2019). Periodic event-triggered sampling and dual-rate control for a wireless networked control system with applications to uavs. *IEEE Trans. Ind. Electron.*, 66(4), 3157–3166.

Donkers, M.C.F. and Heemels, W.P.M.H. (2012). Output-based event-triggered control with guaranteed $\mathcal{L}_\infty$-gain and improved and decentralized event-triggering. *IEEE Trans. Autom. Control*, 57(6), 1362–1376.

Groff, L.B., Moreira, L.G., and Gomes da Silva Jr., J.M. (2016). Event-triggered control co-design for discrete-time systems subject to actuator saturation. In *Proceedings of the IEEE Conference on Computer Aided Control System Design*, 1452–1457.

Heemels, W.P.M.H., Donkers, M.C.F., and Teel, A.R. (2013). Periodic event-triggered control for linear systems. *IEEE Trans. Autom. Control*, 58(4), 847–861.

Heemels, W.P.M.H., Johansson, K.H., and Tabuada, P. (2012). An introduction to event-triggered and self-triggered control. In *Proceedings of the IEEE Conference on Decision and Control*, 3270–3285. Maui.

Jia, X.C., Chi, X.B., Han, Q.L., and Zheng, N.N. (2014). Event-triggered fuzzy $H_\infty$ control for a class of nonlinear networked control systems using the deviation bounds of asynchronous normalized membership functions. *Information Sciences*, 259, 100 – 117.

Li, J. and Huang, X. (2017). A switched event-triggered $H_\infty$ control approach to nonlinear network control system. In *Proceedings of the Chinese Control Conference*, 4239–4244. Da lian.

Moreira, L.G., Groff, L.B., Gomes da Silva Jr., J.M., and Coutinho, D. (2017). Event-triggered control for nonlinear rational systems. *IFAC-PapersOnLine*, 50(1), 15307–15312. 20th IFAC World Congress.

Moreira, L.G., Groff, L.B., Gomes da Silva Jr., J.M., and Tarbouriech, S. (2019a). PI event-triggered control under saturating actuators. *Int. J. Control*, 92, 1634–1644.

Moreira, L.G., Tarbouriech, S., Seuret, A., and Gomes da Silva Jr., J.M. (2019b). Observer-based event-triggered control in the presence of cone-bounded nonlinear inputs. *Nonlinear Analysis: Hybrid Systems*, 33, 17 – 32.

Peralez, J., Andrieu, V., Nadri, M., and Serres, U. (2018). Event-triggered output feedback stabilization via dynamic high-gain scaling. *IEEE Trans. Autom. Control*, 63(8), 2537–2549.

Selivanov, A. and Fridman, E. (2016). Event-triggered $H_\infty$ control: A switching approach. *IEEE Trans. Autom. Control*, 61(10), 3221–3226.

Seuret, A., Prieur, C., Tarbouriech, S., and Zaccarian, L. (2016). LQ-based event-triggered controller co-design for saturated linear systems. *Automatica*, 74, 47–54.

Tabuada, P. (2007). Event-triggered real-time scheduling of stabilizing control tasks. *IEEE Trans. Autom. Control*, 52(9), 1680–1685.

Tarbouriech, S., Seuret, A., Moreira, L.G., and Gomes da Silva Jr., J.M. (2017). Observer-based event-triggered control for linear systems subject to cone-bounded nonlinearities. *IFAC-PapersOnLine*, 50(1), 7893–7898. 20th IFAC World Congress.

Tayebi, A. and McGilvray, S. (2006). Attitude stabilization of a VTOL quadrotor aircraft. *IEEE Trans. Control Syst. Technol.*, 14(3), 562–571.

Trofino, A. (2000). Robust stability and domain of attraction of uncertain nonlinear systems. In *Proceedings of the American Control Conference*, volume 5, 3707–3711. New York: IEEE, Chicago.

Wang, W., Postoyan, R., Nešić, D., and Heemels, W.P.M.H. (2018). Periodic event-triggered output feedback control of nonlinear systems. In *2018 IEEE Conference on Decision and Control (CDC)*, 957–962.

Wu, F.X. and Mu, L. (2009). Parameter estimation in rational models of molecular biological systems. In *Proceedings of the Annual International Conference of the IEEE Engineering in Medicine and Biology Society*, 3263–3266. New York: IEEE, Minneapolis.

Xing, L., Wen, C., Liu, Z., Su, H., and Cai, J. (2019). Event-triggered output feedback control for a class of uncertain nonlinear systems. *IEEE Trans. Autom. Control*, 64(1), 290–297.